Role for Heparin-Binding Growth Factors in Glucose-Induced Vascular Dysfunction

Clifford C. Stephan, Katherine C. Chang, Wanda LeJeune, David Erichsen, Robert J. Bjercke, Ajay Rege, Ronald J. Biediger, Timothy P. Kogan†, Tommy A. Brock, Joseph R. Williamson, and Ronald G. Tilton

Vascular hyperpermeability and excessive neovascularization are hallmarks of early and late vascular endothelial cell dysfunction induced by diabetes. Vascular endothelial growth factor (VEGF) appears to be an important mediator for these early and late vascular changes. We reported previously, using skin chambers mounted on backs of SD rats, that neutralizing antibodies directed against VEGF blocked vascular permeability and blood flow changes induced by elevated tissue glucose and sorbitol levels in a dosage-dependent manner. We report in this study, using the same skin chamber model and neutralizing antibodies directed against basic fibroblast growth factor (FGF-2), that another member of the heparin-binding growth factor family also mediates glucose- and sorbitol-induced vascular permeability and blood flow increases. In addition, we show that *1*) TBC1635, a novel heparin-binding growth factor antagonist, blocks the vascular hyperpermeability and blood flow increases induced by elevated tissue levels of glucose and sorbitol and by topical application of VEGF and FGF-2 to granulation tissue in skin chambers, and *2*) suramin, a commercially available growth factor antagonist, blocks glucose-induced vascular dysfunction. These results suggest an early role for heparin-binding growth factors in the vascular dysfunction caused by excessive glucose metabolism, possibly via the sorbitol pathway. *Diabetes* 47:1771–1778, 1998

Diabetic vascular injury is characterized acutely by leakage of plasma constituents and more chronically by vascular structural changes, including excessive neovascularization, in addition to hyperpermeability. Results of recent studies have suggested that vascular endothelial growth factor (VEGF), an endothelial cell-specific mitogen linked to angiogenesis through its effect on endothelial cell proliferation, migration, and tube formation (1–4), mediates the neovascularization associated with proliferative diabetic retinopathy. The intravitreal concentration of VEGF correlates closely with neovascularization not only in patients with diabetic retinopathy (5–8) but also in other retinal disorders characterized by excessive neovascularization (9–12). Intravitreal injection of VEGF inhibitors (*flt*- and *flk*-IgG chimeric proteins, antibodies directed against VEGF, and antisense oligodeoxynucleotides directed against VEGF mRNA) can block intraocular angiogenesis in a variety of animal models of neovascularization (13–15).

VEGF also displays other biologically relevant activities, such as the ability to increase vascular permeability (16) and induce vascular relaxation (17), possibly through mechanisms involving protein kinase C (PKC) activation (18), increased nitric oxide production (19,20), and platelet-activating factor synthesis (21). We have reported that the vascular hyperpermeability and increased blood flow caused by elevated tissue glucose and sorbitol levels can be blocked by neutralizing monoclonal and polyclonal antibodies directed against VEGF (20), suggesting that sorbitol pathway-linked increases in VEGF may be involved in the hemodynamic changes and loss of endothelial cell barrier integrity induced by diabetes. Recent reports that acute exposure of vascular smooth muscle cells (22,23), retinal pigment epithelial cells (24), and rat glial tumor cells (25) to elevated glucose levels in tissue culture increases VEGF mRNA and protein content, together with reports that glycated proteins increase VEGF in cultured retinal Müller cells (26), suggest that VEGF plays an early, permissive role in the pathogenesis of diabetic vascular dysfunction.

VEGF is one member of a family of heparin-binding growth factors that also includes platelet-derived growth factor, the fibroblast growth factors (FGFs), and heparin-binding epidermal growth factor (hbEGF). Basic fibroblast growth factor (FGF-2), like VEGF, is recognized as a potent endothelial cell mitogen and angiogenic factor. Threefold increases in FGF-2 mRNA levels have been reported in eyes of streptozotocin-induced diabetic rats (27) and in rat aortic smooth muscle cells exposed to 30 mmol/l glucose in tissue culture (28). Likewise, significant increases in FGF-2 protein have been reported in the vitreous of patients with proliferative diabetic retinopathy (29,30) and in the serum of pregnant diabetic women with retinopathy in 2nd and early 3rd trimesters (31). Although there are numerous reports that levels of other members of this growth factor family are elevated in diabetes (32–36), it remains unclear if these changes in

From the Departments of Cell Biology (W.L., R.G.T.), Pharmacology (C.C.S., D.E., A.R., T.A.B.), Immunology (R.J.Bj.), and Chemistry and Biophysics (R.J.Bi., T.P.K.), Texas Biotechnology Corporation, Houston, Texas; and the Department of Pathology (K.C.C., J.R.W.), Washington University School of Medicine, St. Louis, Missouri.

Address correspondence and reprint requests to Dr. Ronald G. Tilton, Department of Cell Biology, Texas Biotechnology Corporation, 7000 Fannin, Houston, TX 77030. E-mail: rtilton@tbc.com.

Received for publication 18 March 1998 and accepted in revised form 29 July 1998.

C.C.S., W.L., D.E., R.J.Bj., A.R., R.J.Bi., T.A.B., and R.G.T. own stock in Texas Biotechnology Corporation.

†Deceased May 1998.

BSA, bovine serum albumin; EGF, epidermal growth factor; FGF, fibroblast growth factor; hbEGF, heparin-binding EGF; HUVEC, human umbilical vein endothelial cell; mAb, monoclonal antibody; PBS, phosphate-buffered saline; PKC, protein kinase C; PLC, phospholipase C; PLSD, protected least significant difference; TGF-α, transforming growth factor-α; VEGF, vascular endothelial growth factor.

growth factor levels, including FGF-2, are causally linked to the vascular dysfunction induced by diabetes.

In the present experiments, we demonstrated that a monoclonal antibody (mAb) directed against FGF-2 can significantly attenuate glucose- and sorbitol-induced vascular dysfunction. In addition, we report that TBC1635, a heparin-binding growth factor antagonist, blocks albumin hyperpermeability and blood flow increases induced by VEGF and FGF-2 and by elevated tissue levels of glucose and sorbitol. We further report that suramin, a commercially available growth factor antagonist, also blocks glucose-induced vascular changes. These data indicate that accelerated glucose metabolism, possibly via the sorbitol pathway, increases the expression/activity of heparin-binding growth factors sufficiently to cause vascular dysfunction.

RESEARCH DESIGN AND METHODS

Animals and materials. Male SD rats (~225 g) were purchased from Sasco (Indianapolis, IN) and female BALB/c mice were purchased from Harlan Sprague Dawley (Indianapolis, IN). Housing and anesthesia concurred with the guidelines established by the Washington University and University of Texas Health Science Center Institutional Animal Welfare Committees and in accordance with the Public Health Service Guide for the Care and Use of Laboratory Animals, U.S. Department of Agriculture regulations, and the American Veterinary Medicine Association's Panel on Euthanasia guidelines. Rats were housed individually, were fed standard rat diet (Standard Laboratory Rodent Diet No. 5001; Ralston Purina, Richmond, IN) and water ad libitum, and were on a 12-h light/dark cycle. ^{125}I and ^{46}Sc microspheres were obtained from Du Pont-NEN (Boston, MA). ^{131}I was obtained from ICN Biomedicals (Costa Mesa, CA). Unless stated otherwise, all other chemicals and reagents were obtained from Sigma (St. Louis, MO) and were of the highest grade available.

Preparation and characterization of TBC254F1, a neutralizing monoclonal FGF-2 antibody. Five female BALB/c mice aged 8 weeks were immunized by intraperitoneal and subcutaneous injections of 50 µg recombinant human fibroblast growth factor (rhFGF)-2 per mouse in complete Freund's adjuvant (Sigma), then boosted twice, 21 days apart, using incomplete Freund's adjuvant. The two mice with the highest serum level of anti-rhFGF-2 and neutralizing antibody activity were injected intravenously with an additional 30 µg of immunogen in phosphate-buffered saline (PBS) 21 days after the last immunization. Then, 3 days later, spleen cells of each mouse were harvested for production of hybridomas to human recombinant FGF-2 using previously described techniques (37), as modified by Bjercke et al. (38). mAb TBC254F1 gave the highest antibody titer and neutralizing antibody activity; these hybridoma cells were cloned four times by limiting dilution in 96-well microtiter plates. The cloned hybridomas (10^7 cells) were injected intraperitoneally into BALB/c mice that had been primed with pristane 2 weeks earlier. After 7–10 days, ascites fluid was collected and pooled; purified IgG was prepared by protein A chromatography, then stored at –80°C. The isotype and light-chain composition of the cloned mAb was determined using enzyme-linked immunosorbent assay (ELISA) (R&D Systems, Minneapolis, MN), substituting secondary antibody reagents with alkaline phosphatase conjugated rabbit IgG antibodies specific for mouse IgG_1, IgG_{2a}, IgG_{2b}, IgG_3, IgM, or mouse κ or λ light chains.

Binding studies were performed as detailed below using the human FGF receptor (*flg*) extracellular domain fused to the heavy chains of a mouse IgG_{2a} antibody, then captured onto Immulon 4 strip wells (Dynatech Laboratories, Chantilly, VA) with IgG_{2a}-specific goat anti-mouse antibody. Increasing concentrations of monoclonal FGF-2 antibody were incubated separately with 3 ng/ml ^{125}I-labeled FGF-2 (Biomedical Technologies, Stoughton, MA) before being added to the receptor. Nonspecific binding was defined as the binding measured in the presence of a 100-fold molar excess of unlabeled FGF-2.

Characterization of TBC1635

Receptor binding assays. The ability of TBC1635 to block growth factor–receptor interaction was evaluated using the heparin-binding growth factors VEGF, FGF-1, FGF-2, and hbEGF. Epidermal growth factor (EGF), a non-heparin-binding growth factor, was used as a negative control. Binding studies were performed using *1*) the seven-loop ectodomain of human *flt*-1 fused to the heavy chains of a mouse IgG_{2a} antibody for VEGF, *2*) the two-loop ectodomain of human *flg* receptor fused to the heavy chains of a mouse IgG_{2a} antibody for FGF-1 and FGF-2, and *3*) the extracellular domain of recombinant human EGF receptor (Austral Biologicals, San Ramon, CA) for hbEGF and EGF. Both fusion proteins were made in-house by cloning the respective receptors into a vector containing the heavy chains of the mouse IgG_{2a} for use in a baculovirus expression system. Insect cells (sf-21) were grown in T-175 flasks (Falcon, Franklin Lakes, NJ) in SFM-900 II serum-free growth medium (Gibco BRL, Gaithersburg, MD) for 2–3 days after infection with virus. The *flt*- and *flg*-fusion proteins were captured from the culture media onto Immulon-4 strip wells (Dynatech) precoated overnight with 1 µg/ml IgG_{2a}-specific goat anti-mouse antibody (Southern Biotechnology, Birmingham, AL) in PBS at 4°C. The recombinant human epidermal growth factor (rhEGF) soluble receptor (10 ng/well in PBS) was coated directly onto Immulon-4 wells overnight at 4°C. TBC1635 was added to individual wells at a concentration of 10 µmol/l together with one of the following in a total volume of 150 µl/well: *1*) 4 ng/ml ^{125}I-labeled VEGF (Biomedical Technologies), *2*) 3 ng/ml ^{125}I-labeled FGF-1 or ^{125}I-labeled FGF-2, and *3*) 3 ng/ml ^{125}I-labeled EGF (Biomedical Technologies) or ^{125}I-labeled hbEGF (iodinated in-house using the Iodobead method with ^{125}I obtained from Du Pont-NEN). Incubations were terminated after 90 min at 22°C by washing the wells three times with 200 µl of ice-cold PBS. Nonspecific binding was defined as the binding measured in the presence of a 100-fold molar excess of unlabeled growth factor. Unlabeled, carrier-free human recombinant FGF-1 and FGF-2 were obtained from Peprotech (Princeton, NJ); human recombinant EGF and hbEGF were obtained from R&D Systems (Minneapolis, MN). Bound growth factor activity was measured in a Genesys γ counter (Life Technology, Schaumburg, IL); results were expressed as the percentage inhibition of total specific counts in control wells. In a separate experiment, a binding study was performed with increasing concentrations of TBC1635 (10^{-10} to 10^{-2} mol/l TBC1635) incubated with 3 ng/ml ^{125}I-FGF-2, as detailed above.

Signaling assays

VEGF-induced intracellular Ca^{2+} changes in human umbilical vein endothelial cell. A Ca^{2+}-sensitive fluorescent dye, fura-2 (Molecular Probes, Eugene, OR), was used to monitor changes in intracellular Ca^{2+} levels in human umbilical vein endothelial cell (HUVEC) suspensions in response to exogenous VEGF, as previously described (39). HUVECs were plated at 12,500 cells/cm^2 in 100-mm gelatin-coated plates (Falcon) and maintained in M199 culture medium containing 15% fetal bovine serum, 10 µmol/l thymidine, 2 µmol/l glutamine, 100 U/ml penicillin, 100 µg/ml streptomycin, 50 µg/ml endothelial cell mitogen (Biomedical Technologies), and 100 µg/ml heparin for 3–5 days (80–90% confluent). Cells were removed with PBS (lacking Ca^{2+} and Mg^{2+}) containing 2 µmol/l EDTA, washed with PBS containing 0.1% bovine serum albumin (BSA), then loaded with 2 µmol/l of the cell permeant acetoxymethylester derivative of fura-2 for 20 min at 37°C. TBC1635 (50–300 nmol/l) was incubated with the fura-2–loaded cells (5×10^5 in 2 ml PBS) for 10 min at 37°C before the addition of recombinant human vascular endothelial growth factor (rhVEGF) (10 ng/ml final concentration). Fura-2 fluorescence was monitored with a Photon Technologies fluorometer (South Brunswick, NJ) at 340 and 380 nm and calibrated using digitonin (0.25 mmol/l) and EGTA (10 mmol/l, pH 12.0) to obtain maximum and minimum fluorescence signals, respectively. Intracellular Ca^{2+} concentrations ($[Ca^{2+}]_i$) were calculated using the following formula: $[Ca^{2+}]_i = K_d(R - R_{min})/(R_{max} - R) \times (EGTA_{380}/DIG_{380})$ as previously described (39), in which K_d is the dissociation constant, R is fluorescence signal, and DIG is digitonin.

Inhibition of FGF-2–induced phospholipase C–γ phosphorylation in NIH 3T3 cells. NIH 3T3 cells were grown to 75% confluence in Dulbecco's modified Eagle's medium (DMEM) containing 15% bovine calf serum (BCS), then growth-arrested for 24 h in DMEM containing 0.5% BCS. After a 45-min incubation at 37°C with a physiologically balanced salt solution containing 100 µmol/l sodium orthovanadate to inhibit endogenous phosphatase activity, cells were incubated with 1, 10, or 100 µmol/l TBC1635 at 37°C for 15 min, followed by induction of signaling with FGF-2 (25 ng/ml, 37°C, 30 min) in the presence of the inhibitor. Cells were lysed by the addition of 100 µl cold lysis buffer; released phospholipase C–γ (PLC-γ) was immunoprecipitated with an anti–PLC-γ antibody (Upstate Biotechnology; Lake Placid, NY) attached to protein A–sepharose beads (Pharmacia Biotech, Piscataway, NJ); and proteins were separated by denaturing polyacrylamide gel electrophoresis and were transferred electrophoretically to a polyvinyledene fluoride membrane. Phosphorylated PLC-γ was visualized with chemiluminescence using an anti-phosphotyrosine antibody (Transduction Laboratories, Lexington, KY). PLC-γ phosphorylation was quantitated by scanning densitometry.

Granulation tissue skin chamber. A modification of the skin chamber model used by Lundberg and Gerdin (40), as described previously (20,41), was used in these studies. Briefly, hair was shaved from the upper back of pentobarbital sodium–anesthetized rats (35 mg/kg body wt, i.p.) and 2-cm circles of skin were removed from either side of the midline. The flanged base of the plastic chamber was sutured to the skin at the margins of the wound with the skin overlapping the flange. Granulation tissue containing new vessels formed on the surface of the exposed fascia inside the chamber. The chambers were equipped with stainless steel screwcaps that could be removed to permit addition of pharmacological agents to the granulation tissue.

Measurement of vascular albumin permeation and blood flow in granulation tissue. Vascular albumin permeation (^{125}I-labeled BSA clearance, expressed as µg plasma · g^{-1} tissue wet wt · min^{-1}) and blood flow (ml · g^{-1} tissue wet wt ·

min^{-1}) were quantified using a double isotope–dilution technique and radiolabeled microspheres, respectively, in thiopental-anesthetized rats (65 mg/kg body wt, i.p.), as described previously in detail (42,43). ^{125}I-labeled BSA was used to quantify vascular albumin permeation after 10 min of tracer circulation, and ^{131}I-labeled BSA served as a plasma volume marker for correction of ^{125}I -BSA tissue activity for tracer contained within vessels. Very briefly, ^{125}I-BSA activity in granulation tissue was corrected for tissue intravascular content of this tracer by subtracting the product of ^{131}I-BSA tissue activity multiplied by the ratio of ^{125}I-BSA to ^{131}I-BSA activity in the arterial plasma sample obtained at the end of the experiment. Vascular-corrected ^{125}I-BSA activity was divided by the time-averaged ^{125}I-BSA plasma activity (obtained from a well-mixed sample of plasma taken from the withdrawal syringe) and by the tracer circulation time (10 min) and then normalized per gram of tissue wet weight. Granulation tissue blood flow was assessed with 11.3 µm ^{46}Sc microspheres using conventional reference tracer techniques.

Experimental protocols

FGF-2 antibody inhibition of glucose-induced vascular dysfunction. Seven days after insertion of the chambers, 1.5 ml of HEPES buffer (25 mmol/l HEPES [pH 7.4], 137 mmol/l NaCL, 4.2 mmol/l KCL, 3 mmol/l Na_2HPO_4, 100 µg/ml penicillin G, 10 µg/ml gentamicin, 2% polyvinylpyrrolidone) plus one of the following reagents was added to individual chambers: *1*) 5 mmol/l D-glucose, *2*) 5 mmol/l D-glucose + 30 µg/ml TBC254F1 mAb, *3*) 30 mmol/l D-glucose, *4*) 30 mmol/l D-glucose + 30 µg/ml TBC254F1 antibody, *5*) 30 mmol/l D-glucose + 100 µg/ml TBC254F1 antibody, or *6*) 30 mmol/l D-glucose + 100 µg/ml nonspecific rabbit antibody. These solutions were added twice daily (9:00 A.M. and 5:00 P.M.) for 7 days. Albumin clearance and blood flow were assessed within 1 h of the final treatment.

Inhibition of glucose- and sorbitol-induced vascular dysfunction with TBC1635. Seven days after insertion of the chambers, 1.5 ml of HEPES buffer plus one of the following reagents was added to individual chambers: *1*) 5 mmol/l D-glucose, *2*) 5 mmol/l D-glucose + 100 µmol/l TBC1635, *3*) 30 mmol/l D-glucose, *4*) 30 mmol/l D-glucose + 10 µmol/l TBC1635, *5*) 30 mmol/l D-glucose + 30 µmol/l TBC1635, *6*) 30 mmol/l D-glucose + 100 µmol/l TBC1635, *7*) 1 mmol/l sorbitol, or *8*) 1 mmol/l sorbitol + 100 µmol/l TBC1635. These solutions were added twice daily (9:00 A.M. and 5:00 P.M.) for 7 days. Within 1 hour of the final treatment, albumin clearance and blood flow were assessed as detailed above. DMSO (1%) was used to solubilize TBC1635, and appropriate controls in the presence of 5 and 30 mmol/l glucose were evaluated after 7 days of treatment in granulation tissue. In separate experiments, 30 mmol/l glucose ± 100 µmol/l suramin and 1 mmol/l sorbitol ± 100 µg/ml TBC254F1 were added twice a day for 7 days, as detailed above.

Inhibition of growth factor–induced vascular dysfunction with TBC1635. Acute experiments evaluating effects of single, topical application of VEGF or FGF-2 were initiated 14 days after mounting tissue chambers. In these studies, 2 ml of HEPES buffer containing 4 ng/ml VEGF ± 100 µmol/l TBC1635 or 50 ng/ml FGF-2 ± 100 µmol/l TBC1635 were applied topically to the granulation tissue, and albumin clearance and blood flow were assessed 1 and 2 h later, respectively.

Statistical analysis. All results in figures and tables are expressed as means ± SD of untransformed data. Overall differences among experimental groups for each parameter were first assessed by one-way analysis of variance (ANOVA), and individual pairwise group comparisons were analyzed by Fisher's protected least significant difference (PLSD) post hoc test only if the ANOVA test was significant at $P < 0.05$ for a given parameter. For the post hoc tests, $P < 0.01$ was considered significant.

RESULTS

TBC1635 and TBC254F1 mAb characterization. The structure of TBC1635 is shown in Fig. 1; it consists of two lysine residues (acid or ester) separated by a pentylene spacer. Two sulfolithocolic acid residues having the structure shown in Fig. 1 are attached via their carboxylic acids to the two free amino groups of each lysine molecule. The molecular weight of TBC1635 as a tetrasodium salt is 2,201.

TBC1635 at a concentration of 10 µmol/l blocked FGF-1 and FGF-2 binding to the *flg*-fusion protein by 76 and 81%, respectively, and blocked VEGF and hbEGF binding to their corresponding receptors by 94 and 89%, respectively (Table 1). Binding of the non-heparin-binding EGF to the EGF receptor was unaffected by TBC1635. In a separate experiment, a complete dosage-response curve was generated for TBC1635 inhibition of FGF-2 binding to the *flg*-fusion protein (Fig. 2*A*). In these experiments, TBC1635 was slightly less effective, with 61% inhibition of binding at 10 µmol/l and an IC_{50} (concentration resulting in 50% inhibition) value of 2 µmol/l. TBC254F1, an anti-FGF-2 mAb, inhibited ^{125}I-FGF-2 binding to the *flg*-fusion protein in a dosage-dependent manner, with a half-maximal inhibition at 10 ng/ml (Fig. 2*B*).

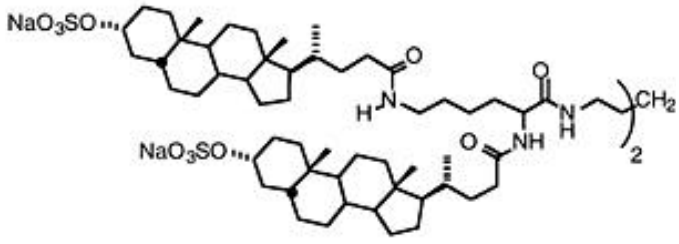

FIG. 1. Molecular structure of TBC1635.

FGF-2–induced PLC-γ phosphorylation in NIH-3T3 cells was inhibited by ~50% with 1 µmol/l TBC1635 and by 100% with 10 µmol/l TBC1635 (Fig. 2*C*). An increased fura-2 signal was evident 20–30 s after the addition of 10 ng/ml rhVEGF to human endothelial cells in suspension, reaching a fourfold increase after 60 sec, then slowly decaying over the remainder of the experiment to a level approximately three times the baseline level (Fig. 3). The VEGF-induced increase in the fura-2 signal in HUVECs was inhibited 100% by 300 nmol/l TBC1635, whereas lower dosages significantly, but in a dosage-dependent manner, delayed a rise in the signal.

A single topical application of VEGF (4 ng/ml) or FGF-2 (50 ng/ml) to granulation tissue in skin chambers produced significant increases in ^{125}I-albumin permeation and blood flow, although it was necessary to use ~12 times more FGF-2 than VEGF and to expose the granulation tissue twice as long to FGF-2 than VEGF (Fig. 4). Co-administering TBC1635 (100 µmol/l) with VEGF and FGF-2 blocked albumin hyperpermeability and blood flow increases induced by these growth factors.

Glucose-induced permeability/blood flow increases were attenuated by TBC254F1. ^{125}I-albumin permeation and blood flow were increased 2.7- and 3-fold by 30 vs. 5 mmol/l glucose controls, respectively ($P < 0.0001$ for both) (Fig. 5). Both the increased albumin permeation and blood flow were attenuated by ~50% when 30 µg/ml TBC254F1 was co-administered with 30 mmol/l glucose and by >85% with 100 µg/ml TBC254F1 ($P < 0.0001$ vs. 30 mmol/l glucose for both). The FGF-2 antibody at a concentration of 30 µg/ml had no effect on albumin permeation when co-administered with 5 mmol/l glucose, although blood flow was increased ~50% ($P < 0.0001$ vs. 5 mmol/l glucose control). An isotype-matched, nonspecific rabbit antibody (100 µg/ml) did not

TABLE 1
Receptor binding assays for characterization of TBC1635

Receptor	Ligand	% Inhibition	TBC1635 concentration (µmol/l)	*n*
flg-IgG	^{125}I-FGF-1	76 ± 11	10	2
	^{125}I-FGF-2	81 ± 14	10	4
flt-IgG	^{125}I-VEGF	94 ± 11	10	2
EGFR	^{125}I-EGF	0	10	2
	^{125}I-hbEGF	89 ± 9	10	2

EGFR, epidermal growth factor receptor.

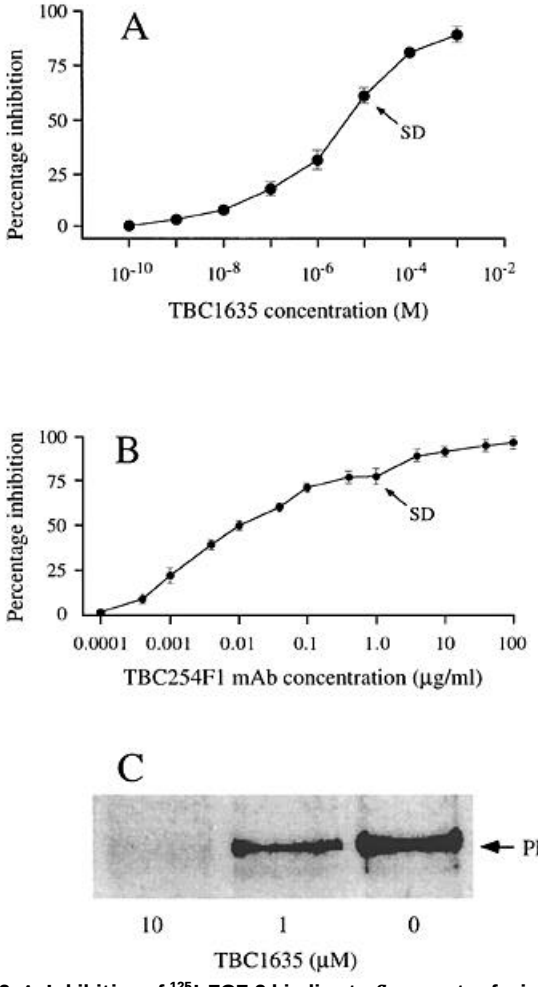

FIG. 2. *A*: Inhibition of ^{125}I-FGF-2 binding to *flg* receptor fusion protein by increasing concentrations of TBC1635. *B*: Inhibition of ^{125}I-FGF-2 binding to *flg* receptor fusion protein by increasing concentrations of the anti-FGF-2 mAb, TBC254F1. For both *A* and *B*, the data plotted represent means ± SD of three separate experiments, with each TBC1635 or antibody concentration measured in duplicate in each experiment. *C*: Representative Western blot showing dosage-dependent inhibition of 25 ng/ml FGF-2-induced PLC-γ phosphorylation in NIH 3T3 cells by TBC1635.

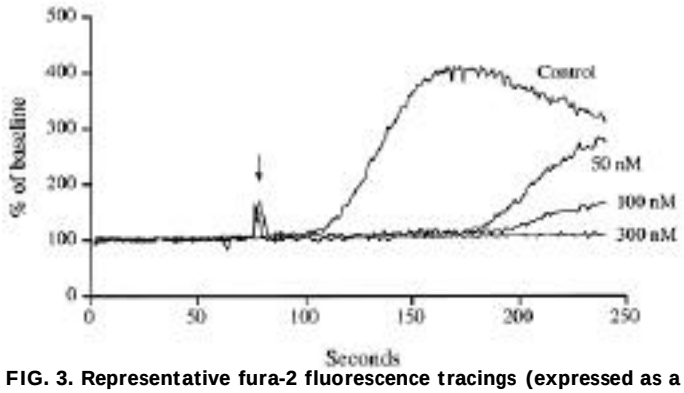

FIG. 3. Representative fura-2 fluorescence tracings (expressed as a percentage of baseline) demonstrating the dosage-dependent prevention of 10 ng/ml VEGF-induced calcium release within human endothelial cells in suspension by TBC1635 (50–300 nmol/l). Application of VEGF is indicated by the arrow.

affect the vascular changes induced by 30 mmol/l glucose. Twice-a-day topical application of 30 mmol/l glucose for 5 days did not increase FGF-2 levels in granulation tissue measured by ELISA; 6 ± 2 ng FGF-2 were measured in granulation tissue treated with both 5 and 30 mmol/l glucose (granulation tissue wet weights averaged ~160 and 180 mg, respectively).

Glucose- and sorbitol-induced permeability and blood flow increases were blocked with TBC1635. The increased albumin permeation and blood flow induced by twice-a-day topical application of 30 mmol/l glucose for 7 days were decreased in a dosage-dependent manner by co-administering TBC1635 with the glucose (Fig. 6). Both the vascular hyperpermeability and blood flow increases were reduced by ~45% and >90% with 30 and 100 μmol/l TBC1635, respectively. Likewise, 100 μmol/l suramin prevented the ^{125}I-albumin permeability and blood flow increases induced by 30 mmol/l glucose. The 1% DMSO used to solubilize TBC1635 did not affect albumin permeation (191 ± 16 and 437 ± 13 μg plasma · min^{-1} · g^{-1} wet wt for 5 and 30 mmol/l glucose, respectively) or blood flow (0.15 ± 0.03 and 0.47 ± 0.01 ml · min^{-1} · g^{-1} wet wt for 5 and 30 mmol/l glucose, respectively).

Twice-a-day topical application of 1 mmol/l sorbitol to granulation tissue for 7 days increased ^{125}I-albumin permeation by 2.7 fold and blood flow by 3.1-fold ($P < 0.0001$ for both vs. 5 mmol/l glucose) (Fig. 7). Co-administering 100 μmol/l TBC1635 with the sorbitol decreased albumin hyperpermeability by 68% and blood flow increases by 79% ($P < 0.0001$ for both vs. 30 mmol/l glucose). Co-administering 100 μg/ml TBC254F1 with the sorbitol decreased albumin hyperpermeability and blood flow increases by ~50% ($P < 0.0001$ for both vs. 30 mmol/l glucose).

DISCUSSION

These experiments demonstrated that vascular dysfunction induced by elevated tissue glucose levels can be attenuated in a dosage-dependent manner by a neutralizing mAb to FGF-2. Together with our previous observation that neutralizing monoclonal and polyclonal VEGF antibodies block glucose- and sorbitol-induced vascular dysfunction (20), these findings suggest that metabolic imbalances linked to elevated tissue glucose levels modulate the activity of heparin-binding growth factors sufficiently to cause vascular dysfunction. Additional support for this suggestion is provided by the demonstration that *1*) a novel, heparin-binding growth factor antagonist, TBC1635, blocked glucose- and sorbitol-induced vascular permeability and blood flow increases in a dosage-dependent manner as well as the same increases induced acutely by a single topical application of FGF-2 or VEGF to the granulation tissue in skin chambers, and *2*) suramin, a polysulfonated napthylurea used as a growth factor antagonist (44–47) and currently under clinical evaluation for the treatment of advanced prostate cancer, completely blocks the vascular dysfunction induced by glucose in the granulation tissue chamber model. Although an important implication of these findings is that heparin-binding growth factors play a role early in the pathogenesis of vascular hyperpermeability and hemodynamic changes induced by diabetes, extrapolating these results to diabetic vascular dysfunction in tissues that are sites of complications must be done cautiously, since the response of vessels in developing granulation tissue may be uniquely sensitive to FGF-2 and differ from the response of

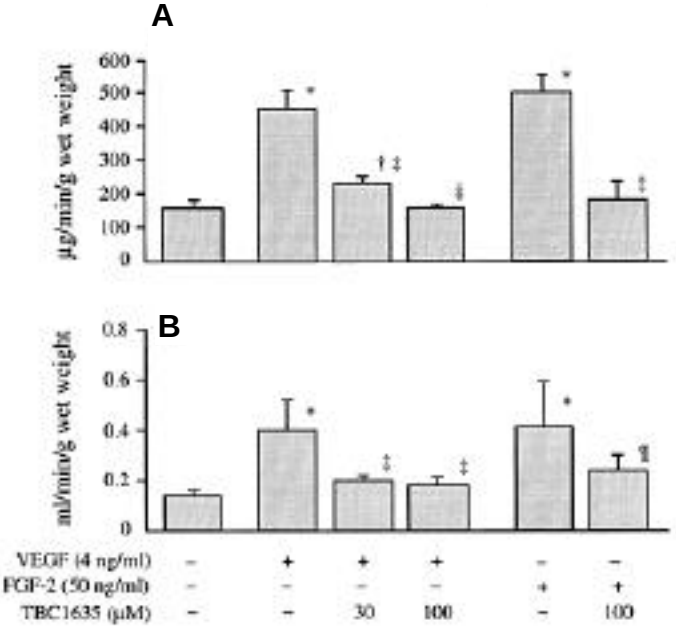

FIG. 4. Effects of TBC1635 on VEGF- and FGF-2–induced increases in ^{125}I-albumin permeation (A) and blood flow (B) in granulation tissue. Controls (5 mmol/l glucose), n = 16; VEGF, n = 7; VEGF + 30 µg/ml TBC1635, n = 5; VEGF + 100 µg/ml TBC1635, n = 6; FGF-2, n = 8; FGF-2 + 100 µg/ml TBC1635, n = 3. Results are means ± SD. *P < 0.0001, †P < 0.001, pairwise comparisons vs. control values; ‡P < 0.0001; ¶P < 0.01 vs. VEGF and FGF-2 values (all comparisons by Fisher's PLSD post hoc test).

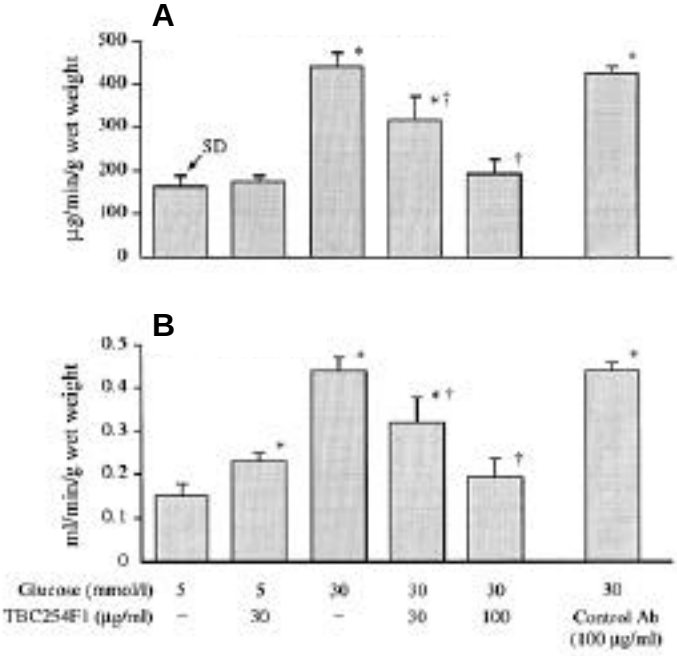

FIG. 5. Effects of neutralizing FGF-2 mAb, TBC254F1, on glucose-induced increases in ^{125}I-albumin permeation (A) and blood flow (B) in granulation tissue: 5 mmol/l glucose, n = 22; 5 mmol/l glucose + 30 µg/ml TBC254F1, n = 5; 30 mmol/l glucose, n = 20; 30 mmol/l glucose + 30 µg/ml TBC254F1, n = 9; 30 mmol/l glucose + 100 µg/ml TBC254F1, n = 5; 30 mmol/l glucose + 100 µg/ml control Ab, n = 4. Results are means ± SD. *P < 0.0001, pairwise comparisons vs. 5 mmol/l glucose control values; †P < 0.0001 vs. 30 mmol/l untreated glucose values (all comparisons by Fisher's PLSD post hoc test).

more mature vessels. However, interventions that modulate vascular hyperpermeability in skin chamber granulation tissue in response to glucose or sorbitol have the same effect in retina, aorta, and sciatic nerve of diabetic animals. This observation supports the likelihood that the pathophysiological mechanisms involved in the hyperpermeability and hemodynamic changes are not unique to the granulation tissue.

The finding that FGF-2 increases granulation tissue blood flow, albeit more slowly and at higher dosages than VEGF, is consistent with several reports that FGF-2 can vasodilate different tissue vasculatures (48–50). The observation that FGF-2 also increases vascular albumin permeability in granulation tissue appears to be novel. The mechanism(s) by which FGF-2 increases tissue blood flow (and vascular permeability) remains unclear, but may involve increases in cytosolic calcium (51,52) and activation of endothelial nitric oxide synthase (49,50,53,54). This is consistent with evidence indicating that VEGF also exerts its hyperpermeability and hemodynamic effects on vascular endothelium via changes in intracellular calcium and nitric oxide (17,19,20). It is an interesting but unexplained phenomenon that both the monoclonal anti-FGF-2 antibody and TBC1635 increased granulation tissue blood flow in controls (Figs. 5 and 6), a phenomenon that was not observed with anti-VEGF antibodies.

Binding of FGF-2 and VEGF to their respective receptors—which have been identified as transmembrane glycoproteins with an extracellular ligand-binding domain consisting of a variable number of immunoglobulin-like domains, a single transmembrane-spanning domain, and an intracellular tyrosine kinase domain—activates protein tyrosine kinase activity; cellular target proteins such as PLC-γ also become phosphorylated. This catalyzes the hydrolysis of phosphatidylinositol, generating diacylglycerol and free inositol phosphate, which, in turn, activates PKC and increases intracellular calcium, respectively. VEGF may mediate its vascular functional changes in the retina via this mechanism, since VEGF-induced retinal hyperpermeability can be blocked by the PKC β-selective inhibitor, LY333531 (18). However, effects of VEGF on vascular hyperpermeability and blood flow also appear to be mediated, at least in part, via increases in intracellular calcium and nitric oxide (17,19,20). Links between VEGF-induced increases in PKC and nitric oxide synthase activities, and the potential for similar mechanisms to account for FGF-2–induced permeability and blood flow changes, remain unclear at this time. Although FGF-2 also induces PLC-γ phosphorylation (Fig. 2C), it may mediate its hyperpermeability effect via signal transduction mechanisms postulated to play a role in its mitogenic and proliferative effects, including activation of phospholipase A_2 and subsequent production of arachidonic acid metabolites (55) or involvement of the phospholipase D pathway via PKC activation (56).

The mechanism(s) by which glucose increases growth factor activity also remains unclear. However, it is noteworthy that increased heparin-binding growth factor mRNA and protein levels have been linked to virtually every biochemical perturbation (associated with elevated tissue glucose levels) postulated to play a role in the pathogenesis of dia-

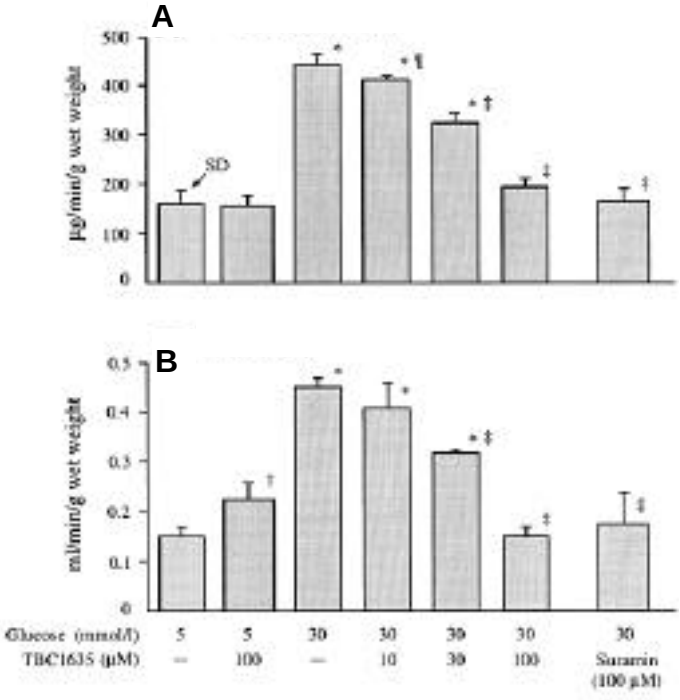

FIG. 6. Effects of TBC1635 on glucose-induced increases in ^{125}I-albumin permeation (A) and blood flow (B) in granulation tissue: 5 mmol/l glucose, n = 12; 5 mmol/l glucose + 100 µmol/l TBC1635, n = 3; 30 mmol/l glucose, n = 12; 30 mmol/l glucose + 10 µmol/l TBC1635, n = 3; 30 mmol/l glucose + 30 µmol/l TBC1635, n = 3; 30 mmol/l glucose + 100 µmol/l TBC1635, n = 3; 30 mmol/l glucose + 100 µmol/l suramin, n = 5. Results are means ± SD. *P < 0.0001, †P < 0.006, pairwise comparisons vs. 5 mmol/l glucose control values; ‡P < 0.0001, ¶P < 0.007 vs. 30 mmol/l untreated glucose values (all comparisons by Fisher's PLSD post hoc test).

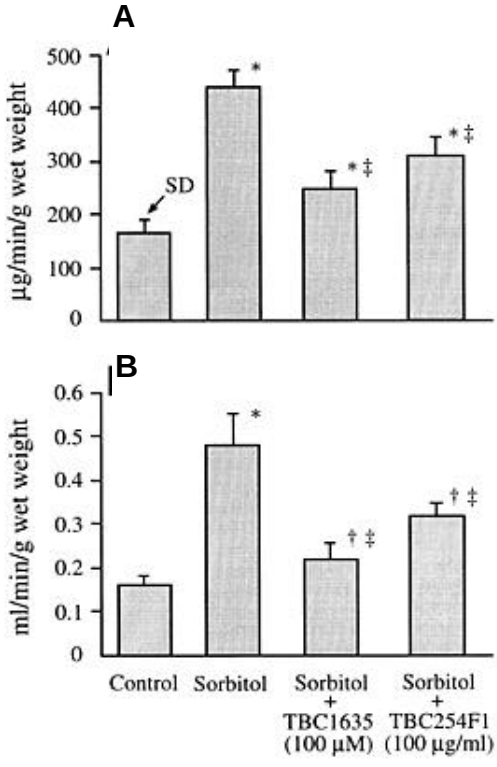

FIG. 7. Effects of TBC1635 and TBC254F1 on sorbitol-induced increases in ^{125}I-albumin permeation (A) and blood flow (B) in granulation tissue: 5 mmol/l glucose, n = 11; 1 mmol/l sorbitol, n = 8; 1 mmol/l sorbitol + 100 µmol/l TBC1635, n = 8; 1 mmol/l sorbitol + 100 µg/ml TBC254F1, n = 5. Results are means ± SD. *P < 0.0001, †P < 0.002, pairwise comparisons vs. 5 mmol/l glucose control values; ‡P < 0.0001 vs. 1 mmol/l sorbitol values (all comparisons by Fisher's PLSD post hoc test).

betic vascular dysfunction, including increases in sorbitol pathway activity (20,57), PKC activity (23,58), glycation reactions (59,60), and glucosamine levels (28). To date, there have been only a few published reports linking increased growth factor expression/activity to increased sorbitol pathway activity. We have reported that sorbitol pathway-linked vascular dysfunction is mediated, at least in part, via VEGF (20) and can be blocked with TBC1635 (Figs. 6 and 7), whereas Frank et al. (57) reported that a marked upregulation of VEGF expression in rats fed a high-galactose diet for 2 years was attenuated by an aldose reductase inhibitor. In the present study, a neutralizing mAb against FGF-2 significantly attenuated both glucose- and sorbitol-induced vascular functional changes, suggesting another potential link between sorbitol pathway and heparin-binding growth factor activities. It has been reported that sorbinil did not block threefold increases in FGF-2 levels in the retina of 3-week streptozotocin-induced diabetic rats (27); however, in that study, retinal sorbitol levels remained elevated threefold and retinal fructose levels were elevated sixfold in the inhibitor-treated diabetic vs. control groups (Table 1 in 27), indicating incomplete inhibition of sorbitol pathway flux. Increased protein glycation also affects the activity of the heparin-binding growth factor family, since *1*) hbEGF is regulated at the transcriptional level by 3-deoxyglucosone, a highly reactive intermediate in glycation reactions (59); *2*) AGE proteins increase the expression of VEGF (26) and can induce angiogenesis in vitro (60); and *3*) glycated rat serum albumin increases vascular permeability and blood flow, changes that can be blocked by a neutralizing antibody to VEGF (61).

Although elevated glucose concentrations may be able to directly stimulate the transcription of heparin-binding growth factor genes via a glucose-response element, we were unable to find a consensus sequence in the promoter region of both rat (62) and human (63) FGF-2 genes as well as the mouse VEGF gene (64) using the glucose-response element that has been characterized for the L-pyruvate kinase and S14 genes, 5′-CACGTG-3′ (65,66). Rat aortic smooth muscle cells grown in 30 mmol/l glucose had a twofold increase in transforming growth factor-α (TGF-α) mRNA compared with cells grown in 5.5 mmol/l glucose (glucosamine was more effective than glucose at increasing TGF-α mRNA and protein) (28). In that study, a glucose-response element in the promoter region of the TGF-α gene was mapped to a 130–base pair segment that included three potential binding sites for the transcription factor Sp1. Although these authors also reported a threefold increase in FGF-2 in response to glucose, they did not report a glucose-response element in this gene.

In conclusion, these findings *1*) provide additional evidence that vascular dysfunction induced by elevated tissue glucose levels is mediated, at least in part, by FGF-2 and VEGF; *2*) indicate a role for excessive growth factor production, possibly linked to increased sorbitol pathway activity, in the pathogenesis of diabetes-induced vascular changes; and *3*) suggest

that inhibition of the heparin-binding growth factor family may have therapeutic utility in preventing early diabetic vascular dysfunction.

ACKNOWLEDGMENTS

This research was supported by National Institutes of Health Grants EY-06600 and HL-39934 (J.R.W.), by the Kilo Diabetes and Vascular Research Foundation, and by the Texas Biotechnology Corporation.

We thank Nemani Rateri and Antoinette Faller for expert assistance with the animal care and Kay Sughrue for the tissue culture work.

The other authors wish to dedicate this manuscript to the memory of Dr. Timothy P. Kogan, who died from complications of diabetes 27 May 1998 at the age of 41 years.

REFERENCES

1. Ferrara N, Houck L, Jakeman L, Leung DW: Molecular and biological properties of the vascular endothelial growth factor family of proteins. *Endocr Rev* 13:18–32, 1992
2. Keck PJ, Hauser SD, Krivi G, Sanzo K, Warren T, Feder J, Connolly DT: Vascular permeability factor: an endothelial cell mitogen related to platelet derived growth factor. *Science* 246:1309–1312, 1989
3. Ferrara N, Davis-Smyth T: The biology of vascular endothelial growth factor. *Endocr Rev* 18:4–25, 1997
4. Ratajska A, Torry RJ, Kitten GT, Kolker SJ, Tomanek RJ: Modulation of cell migration and vessel formation by vascular endothelial growth factor and basic fibroblast growth factor in cultured embryonic heart. *Dev Dyn* 203:399–407, 1995
5. Aiello LP, Avery RL, Arrigg PG, Keyt BA, Jampel HD, Shah ST, Pasquale LR, Thieme H, Iwamoto MA, Park JE, Nguyen HV, Aiello LM, Ferrara N, King GL: Vascular endothelial growth factor in ocular fluid of patients with diabetic retinopathy and other retinal disorders. *N Engl J Med* 331:1480–1487, 1994
6. Adamis A, Miller J, Bernal M-T, D'Amico D, Folkman J, Yeo T-K, Yeo K-T: Increased vascular endothelial growth factor levels in the vitreous of eyes with proliferative diabetic retinopathy. *Am J Ophthalmol* 118:445–450, 1994
7. Malecaze F, Clamens S, Simorre-Pinatel V, Mathis A, Chollet P, Favard C, Bayard F, Plouet J: Detection of vascular endothelial growth factor messenger RNA and vascular endothelial growth factor-like activity in proliferative diabetic retinopathy. *Arch Ophthalmol* 112:1476–1482, 1994
8. Pe'er J, Folberg R, Itin A, Gnessin H, Hemo I, Keshet E: Upregulated expression of vascular endothelial growth factor in proliferative diabetic retinopathy. *Br J Ophthalmol* 80:241–245, 1996
9. Miller JW, Adamis AP, Shima DT, D'Amore PA, Moulton RS, O'Reilly MS, Folkman J, Dvorak HF, Brown LF, Berse B, Yeo T-K, Yeo K-T: Vascular endothelial growth factor/vascular permeability factor is temporally and spatially correlated with ocular angiogenesis in a primate model. *Am J Pathol* 145:574–584, 1994
10. Pierce EA, Avery RL, Foley ED, Aiello LP, Smith LEH: Vascular endothelial growth factor/vascular permeability factor expression in a mouse model of retinal neovascularization. *Proc Natl Acad Sci U S A* 92:905–909, 1995
11. Lopez PF, Sippy BD, Lambert HM, Thach AB, Hinton DR: Transdifferentiated retinal pigment epithelial cells are immunoreactive for vascular endothelial growth factor in surgically excised age-related macular degeneration-related choroidal neovascular membranes. *Invest Ophthalmol Vis Sci* 37:855–868, 1996
12. Stone J, Chan-Ling T, Pe'er J, Itin A, Gnessin H, Keshet E: Roles of vascular endothelial growth factor and astrocyte degeneration in the genesis of retinopathy of prematurity. *Invest Ophthalmol Vis Sci* 37:290–299, 1996
13. Aiello LP, Pierce EA, Foley ED, Takagi H, Chen H, Riddle L, Ferrara N, King GL, Smith LEH: Suppression of retinal neovascularization in vivo by inhibition of vascular endothelial growth factor (VEGF) using soluble VEGF-receptor chimeric proteins. *Proc Natl Acad Sci U S A* 92:10457–10461, 1995
14. Adamis AP, Shima DT, Tolentino MJ, Gragoudas ES, Ferrara N, Folkman J, D'Amore PA, Miller JW: Inhibition of vascular endothelial growth factor prevents retinal ischemia-associated iris neovascularization in a nonhuman primate. *Arch Ophthalmol* 114:66–71, 1996
15. Robinson GS, Pierce EA, Rook SL, Foley E, Webb R, Smith LEH: Oligodeoxynucleotides inhibit retinal neovascularization in a murine model of proliferative retinopathy. *Proc Natl Acad Sci U S A* 93:4851–4856, 1996
16. Dvorak HF, Brown LF, Detmar M, Dvorak AM: Vascular permeability factor/vascular endothelial growth factor, microvascular hyperpermeability, and angiogenesis. *Am J Pathol* 146:1029–1039, 1995
17. Ku DD, Zaleski JK, Liu S, Brock TA: Vascular endothelial growth factor induces EDRF-dependent relaxation in coronary arteries. *Am J Physiol* 265:H586–H592, 1993
18. Aiello LP, Bursell SE, Clermont A, Duh E, Ishii H, Takagi C, Mori G, Ciulla TA, Ways K, Jirousek M, Smith LE, King GL: Vascular endothelial growth factor–induced retinal permeability is mediated by protein kinase C in vivo and suppressed by an orally effective beta-isoform-selective inhibitor. *Diabetes* 46:1473–1480, 1997
19. Wu HM, Huang Q, Yuan Y, Granger HJ: VEGF induces NO-dependent hyperpermeability in coronary venules. *Am J Physiol* 271:H2735–H2739, 1996
20. Tilton RG, Kawamura T, Chang KC, Ido Y, Bjercke RJ, Stephan CC, Brock TA, Williamson JR: Vascular dysfunction induced by elevated glucose levels in rats is mediated by vascular endothelial growth factor. *J Clin Invest* 99:2192–2202, 1997
21. Sirois MG, Edelman ER: VEGF effect on vascular permeability is mediated by synthesis of platelet-activating factor. *Am J Physiol* 272:H2746–H2756, 1997
22. Natarajan R, Bai W, Lanting L, Gonzales N, Nadler J: Effects of high glucose on vascular endothelial growth factor expression in vascular smooth muscle cells. *Am J Physiol* 273:H2224–H2231, 1997
23. Williams B, Gallacher B, Patel H, Orme C: Glucose-induced protein kinase C activation regulates vascular permeability factor mRNA expression and peptide production by human vascular smooth muscle cells in vitro. *Diabetes* 46:1497–1503, 1997
24. Sone S, Kawakami Y, Okuda Y, Kondo S, Hanatani M, Suzuki H, Yamashita K: Vascular endothelial growth factor is induced by long-term high glucose concentration and up-regulated by acute glucose deprivation in cultured bovine retinal pigmented epithelial cells. *Biochem Biophys Res Commun* 221:193–198, 1996
25. Shweiki D, Neeman M, Itin A, Keshet E: Induction of vascular endothelial growth factor expression by hypoxia and by glucose deficiency in multicell spheroids: implications for tumor angiogenesis. *Proc Natl Acad Sci U S A* 92:768–772, 1995
26. Hirata C, Nakano K, Nakamura N, Kitagawa Y, Shigeta H, Hasegawa G, Ogata M, Ikeda T, Sawa H, Nakamura K, Ienaga K, Obayashi H, Kondo M: Advanced glycation end products induce expression of vascular endothelial growth factor by retinal Müller cells. *Biochem Biophys Res Commun* 236:712–715, 1997
27. Lowe WL, Florkiewicz RZ, Yorek MA, Spanheimer RG, Albrecht BN: Regulation of growth factor mRNA levels in the eyes of diabetic rats. *Metabolism* 44:1038–1045, 1995
28. McClain DA, Paterson AJ, Roos MD, Wei X, Kudlow JE: Glucose and glucosamine regulate growth factor gene expression in vascular smooth muscle cells. *Proc Natl Acad Sci U S A* 89:8150–8154, 1992
29. Sivalingam A, Kenney J, Brown GC, Benson WE, Donoso L: Basic fibroblast growth factor levels in the vitreous of patients with proliferative diabetic retinopathy. *Arch Ophthalmol* 108:869–872, 1990
30. Boulton M, Gregor Z, McLeod D, Charteris D, Jarvis-Evans J, Moriarty P, Khaliq A, Foreman D, Allamby D, Bardsley B: Intravitreal growth factors in proliferative diabetic retinopathy: correlation with neovascular activity and glycaemic management. *Br J Ophthalmol* 81:228–233, 1997
31. Hill DJ, Flyvbjerg A, Arany E, Lauszus FF, Klebe JG: Increased levels of serum fibroblast growth factor-2 in diabetic pregnant women with retinopathy. *J Clin Endocrinol Metab* 82:1452–1457, 1997
32. Hamet P, Sugimoto H, Umeda F, Lecavalier L, Franks DJ, Orth DN, Chiasson JL: Abnormalities of platelet-derived growth factors in insulin-dependent diabetes. *Metabolism* 34:25–31, 1985
33. Lee YJ, Shin SJ, Lin SR, Tan MS, Tsai JH: Increased expression of heparin binding epidermal growth-factor–like growth factor mRNA in the kidney of streptozotocin-induced diabetic rats. *Biochem Biophys Res Commun* 207:216–222, 1995
34. Che W, Asahi M, Takahashi M, Kaneto H, Okado A, Higashiyama S, Taniguchi N: Selective induction of heparin-binding epidermal growth factor–like growth factor by methylglyoxal and 3-deoxyglucosone in rat aortic smooth muscle cells: the involvement of reactive oxygen species formation and a possible implication of atherogenesis in diabetes. *J Biol Chem* 272:18453–18459, 1997
35. Inaba T, Ishibashi S, Gotoda T, Kawamura M, Morino N, Nojima Y, Kawakami M, Yazaki Y, Yamada N: Enhanced expression of platelet-derived growth factor-beta receptor by high glucose: involvement of platelet-derived growth factor in diabetic angiopathy. *Diabetes* 45:507–512, 1996
36. Sharp PS: Growth factors in the pathogenesis of diabetic retinopathy. *Diabetes Rev* 3:164–176, 1995
37. Koehler G, Milstein C: Derivation of specific antibody-producing tissue culture

and tumor lines by cell fusion. *Eur J Immunol* 6:511–519, 1976
38. Bjercke RJ, Cook G, Rychlik N, Gjika HB, Vunakis HV, Longone JJ: Stereospecific monoclonal antibodies to nicotine and cotinine and their use in enzyme-linked immunosorbent assays. *J Immunol Methods* 90:203–213, 1986
39. Brock TA, Dvorak HF, Senger DR: Tumor-secreted vascular permeability factor increases cytosolic Ca^{2+} and von Willebrand factor release in human endothelial cells. *Am J Pathol* 138:213–221, 1991
40. Lundberg C, Gerdin B: The inflammatory reaction in an experimental model of open wounds in the rat: the effect of arachidonic acid metabolites. *Eur J Pharmacol* 97:229–238, 1984
41. Wolf BA, Williamson JR, Easom RA, Chang K, Sherman WR, Turk J: Diacylglycerol accumulation and microvascular abnormalities induced by elevated glucose levels. *J Clin Invest* 87:31–38, 1990
42. Pugliese G, Tilton RG, Speedy A, Chang K, Province MA, Kilo C, Williamson JR: Vascular filtration function in galactose-fed versus diabetic rats: the role of polyol pathway activity. *Metabolism* 39:690–697, 1990
43. Tilton RG, Chang K, Nyengaard JR, Van den Enden M, Ido Y, Williamson JR: Inhibition of sorbitol dehydrogenase: effects on vascular and neural dysfunction in streptozocin-induced diabetic rats. *Diabetes* 44:234–242, 1995
44. Middaugh CR, Mach H, Burke CJ, Volkin DB, Dabora JM, Tsai PK, Bruner MW, Ryan JA, Marfia KE: Nature of the interaction of growth factors with suramin. *Biochemistry* 31:9016–9024, 1992
45. Hosang M: Suramin binds to platelet-derived growth factor and inhibits its biological activity. *J Cell Biochem* 29:265–273, 1985
46. Takano S, Gately S, Neville ME, Herblin WF, Gross JL, Engelhard H, Perricone M, Eidsvoog K, Brem S: Suramin, an anticancer and angiosuppressive agent, inhibits endothelial cell binding of basic fibroblast growth factor, migration, proliferation, and induction of urokinase-type plasminogen activator. *Cancer Res* 54:2654–2660, 1994
47. Waltenberger J, Mayr U, Frank H, Hombach V: Suramin is a potent inhibitor of vascular endothelial growth factor: a contribution to the molecular basis of its antiangiogenic action. *J Mol Cell Cardiol* 28:1523–1529, 1996
48. Cuevas P, Carceller F, Ortega S, Zazo M, Nieto I, Gimenez-Gallego G: Hypotensive activity of fibroblast growth factor. *Science* 254:1208–1210, 1991
49. Rosenblatt S, Irikura K, Caday CG, Finklestein SP, Moskowitz MA: Basic fibroblast growth factor dilates rat pial arterioles. *J Cereb Blood Flow Metab* 14:70–74, 1994
50. Kadota O, Ohta S, Kumon Y, Sakaki S, Matsuda S, Sakanaka M: Role of basic fibroblast growth factor in the regulation of rat basilar artery tone in vivo. *Neurosci Lett* 199:99–102, 1995
51. Hackshaw KV, Shi Y: Fibroblast growth factors mobilize peritoneal macrophage intracellular calcium. *Life Sci* 54:661–670, 1994
52. Zhu DL, Herembert T, Caruelle D, Caruelle JP, Marche P: Involvement of calcium channels in fibroblast growth factor-induced activation of arterial cells in spontaneously hypertensive rats. *J Cardiovasc Pharmacol* 23:395–400, 1994
53. Wu HM, Yuan Y, McCarthy M, Granger HJ: Acidic and basic FGFs dilate arterioles of skeletal muscle through a NO-dependent mechanism. *Am J Physiol* 271:H1087–H1093, 1996
54. Kostyk SK, Kourembanas S, Wheeler EL, Medeiros D, McQuillan LP, D'Amore PA, Braunhut SJ: Basic fibroblast growth factor increases nitric oxide synthase production in bovine endothelial cells. *Am J Physiol* 269:H1583–H1589, 1995
55. Sa G, Fox PL: Basic fibroblast growth factor–stimulated endothelial cell movement is mediated by a pertussis toxin–sensitive pathway regulating phospholipase A_2 activity. *J Biol Chem* 269:3219–3225, 1994
56. Ahmed A, Plevin R, Shoaibi MA, Fountain SA, Ferriani RA, Smith SK: Basic FGF activates phospholipase D in endothelial cells in the absence of inositol-lipid hydrolysis. *Am J Physiol* 266:C206–C212, 1994
57. Frank RN, Amin R, Kennedy A, Hohman TC: An aldose reductase inhibitor and aminoguanidine prevent vascular endothelial growth factor expression in rats with long-term galactosemia. *Arch Ophthalmol* 115:1036–1047, 1997
58. Ishii H, Jirousek MR, Koya D, Takagi C, Xia P, Clermont A, Bursell SE, Kern TS, Ballas LM, Heath WF, Stramm LE, Feener EP, King GL: Amelioration of vascular dysfunctions in diabetic rats by an oral PKC beta inhibitor. *Science* 272:728–731, 1996
59. Taniguchi N, Kaneto H, Asahi M, Takahashi M, Wenyi C, Higashiyama S, Fujii J, Suzuki K, Kayanoki Y: Involvement of glycation and oxidative stress in diabetic macroangiopathy. *Diabetes* 45:S81–S83, 1996
60. Yamagishi S, Yonekura H, Yamamoto Y, Katsuno K, Sato F, Mita I, Ooka H, Satozawa N, Kawakami T, Nomura M, Yamamoto H: Advanced glycation end products–driven angiogenesis in vitro: induction of the growth and tube formation of human microvascular endothelial cells through autocrine vascular endothelial growth factor. *J Biol Chem* 272:8723–8730, 1997
61. Ido Y, Chang K, Smith S, Tilton RG, Williamson JR: Vascular dysfunction in granulation tissue induced by glycated albumin is prevented by antibodies against vascular endothelial growth factor and by a selective inhibitor of the β isoform of protein kinase C (Abstract). *Diabetes* 47 (Suppl. 1):A24, 1998
62. Pasumarthi KBS, Jin Y, Cattini PA: Cloning of the rat fibroblast growth factor-2 promoter region and its response to mitogenic stimuli in glioma C6 cells. *J Neurochem* 68:898–908, 1997
63. Abraham JA, Whang JL, Tumolo A, Mergia A, Friedman J, Gospodarowicz D, Fiddes JC: Human basic fibroblast growth factor: nucleotide sequence and genomic organization. *EMBO J* 5:2523–2528, 1986
64. Shima DT, Kuroki M, Deutsch U, Ng Y, Adamis AP, D'Amore PA: The mouse gene for vascular endothelial growth factor: genomic structure, definition of the transcriptional unit, and characterization of transcriptional and post-transcriptional regulatory sequences. *J Biol Chem* 271:3877–3883, 1996
65. Shih HM, Liu Z, Towle HC: Two CACGTG motifs with proper spacing dictate the carbohydrate regulation of hepatic gene transcription. *J Biol Chem* 270:21991–21997, 1995
66. Girard J, Ferre P, Foufelle F: Mechanisms by which carbohydrates regulate expression of genes for glycolytic and lipogenic enzymes. *Annu Rev Nutr* 17:325–352, 1997

Author Queries (please see Q in margin and underlined text)

Q1: Please define rhEGF, rhFGF, and rhVEGF.

Q1a: OK to add hyphen to TGFα? We normally style transforming growth factor-α with a hyphen.

Q3: The numbers in IgG_1 and IgG_3 have been subscripted—change correct?

Q6: Has K_d been correctly defined? Please define R and DIG.

Q7: Redefinition of DMEM okay?

Q8: Does BCS mean fetal calf serum (FCS) or bovine serum albumin (BSA)?

Q9: Spelling of polyvinylpyrrolidone (instead of polyvinylpyrolidone) correct now?

Q9a: Please define IC_{50}.

Q10: Please define EGFR.

Q11: Is the full name for napthylurea “naphthylthiourea”?

Q12: For the unpublished observations, please provide the initials and last names of researchers.